

UNCLASSIFIED

SECURITY INFORMATION

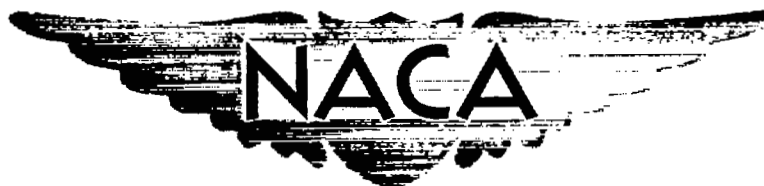
CONFIDENTIAL

Copy
RM E53D22

6

JUN 26 1953

NACA RM E53D22



RESEARCH MEMORANDUM

ALTITUDE PERFORMANCE INVESTIGATION OF A

HIGH-TEMPERATURE AFTERBURNER

By S. C. Huntley, Carmon M. Auble, and James W. Useller

Lewis Flight Propulsion Laboratory
Cleveland, Ohio

CLASSIFICATION CHANGED
UNCLASSIFIED

To

By authority of TPA # 33 Date 10-28-60
ERG

CLASSIFIED DOCUMENT

This material contains information affecting the National Defense of the United States within the meaning of the espionage laws, Title 18, U.S.C., Secs. 793 and 794, the transmission or revelation of which in any manner to an unauthorized person is prohibited by law.

NATIONAL ADVISORY COMMITTEE
FOR AERONAUTICS

WASHINGTON

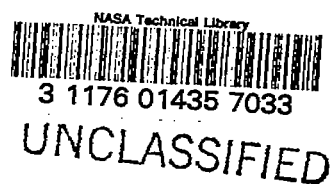
June 26, 1953

NACA LIBRARY

UNCLASSIFIED

CONFIDENTIAL

LABORATORY



NATIONAL ADVISORY COMMITTEE FOR AERONAUTICS

RESEARCH MEMORANDUM

ALTITUDE PERFORMANCE INVESTIGATION OF A HIGH-TEMPERATURE AFTERBURNER

By S. C. Huntley, Carmon M. Auble, and James W. Useller

SUMMARY

An investigation was conducted to ascertain the operational limits of a high-temperature afterburner and to determine its performance over a wide range of flight conditions. Operational limits were obtained at a flight Mach number of 0.8 and performance data were obtained at altitudes from 10,000 to 55,000 feet and flight Mach numbers from 0.6 to 1.0.

A combustion temperature of 3900° R at a combustion efficiency of 0.96 and a corresponding net thrust ratio of 2.03 was obtained for an altitude of 25,000 feet and a flight Mach number of 0.92. Peak combustion temperatures were obtained at the stoichiometric fuel-air ratio or at slightly richer mixtures. Maximum combustion efficiency was reached at a fuel-air ratio of about 0.055 and remained relatively constant with increasing fuel-air ratio. The importance of providing a good fuel distribution by using a large number of injection points rather than relying on penetration was demonstrated by the high burner performance. At the high exhaust-gas temperatures obtained, an excessive amount of air was required to cool the afterburner by the convective shell-cooling method used. As much cooling air as 34 percent of the exhaust-gas flow was required to maintain an average afterburner shell temperature of 1300° F at a combustion temperature of about 3600° R. These requirements stressed the need for a more effective method of utilizing the cooling air for high-temperature afterburners.

INTRODUCTION

The need of military aircraft for greater acceleration rates and higher flight speeds is demanding a more complete exploitation of the thrust potentialities of afterburners. In most previous investigations of afterburning conducted at the NACA Lewis laboratory, the maximum thrust potential of an afterburner was compromised to some extent by afterburner shell cooling. Burning was concentrated in the central portion of the afterburner and the unburned gases in the tail pipe surrounding the high-temperature region were used as a means of

 UNCLASSIFIED

minimizing the secondary air flow required to cool the afterburner shell. The net result was a mean bulk gas temperature somewhat below the maximum that might be expected for a homogeneous stoichiometric fuel-air mixture.

In response to the ever-increasing need for high thrust augmentation, an investigation was conducted that had as its primary objective the attainment of maximum exhaust-gas temperature and thrust (ref. 1). The afterburner shell was supplied with sufficient cooling from an external source to permit high-temperature operation. Performance approaching theoretical values was obtained at a nominal burner inlet pressure of 2450 pounds per square foot by the use of adequate flame-holder blockage, long fuel-mixing length, and relatively low burner-inlet velocity, and by careful matching of the fuel injection pattern to the gas flow pattern to obtain a uniform fuel-air ratio distribution.

Although the afterburners of reference 1 were capable of operation at exhaust-gas temperatures near theoretical, operational limits were not established and performance was obtained for only a limited range of flight conditions. The investigation reported herein was therefore conducted to ascertain the operational limits of the most promising high-temperature afterburner design of reference 1 and to determine its performance over a wide range of flight conditions.

An engine with the aforementioned afterburner was installed in an altitude test chamber at the NACA Lewis laboratory. Operational limits were obtained for a flight Mach number of 0.8 and performance characteristics were determined for a range of altitudes from 10,000 to 55,000 feet and flight Mach numbers from 0.6 to 1.0, which correspond to burner-inlet pressures from 510 to 3090 pounds per square foot. Efforts to further improve the performance of the afterburner led to a brief evaluation of the effect of fuel distribution and certain measurements of the fuel-air ratio distribution within the burner. The cooling requirements of the afterburner were also briefly evaluated.

APPARATUS

Engine

The axial-flow type turbojet engine used in this investigation (fig. 1) develops 3000 pounds thrust at static, sea-level conditions while operating at a rated engine speed of 12,500 rpm with an average turbine-outlet gas temperature of 1625° R. The air flow at this condition is about 58 pounds per second. The engine components consisted of an 11-stage axial-flow compressor, a compressor-outlet mixer, a double-annulus through-flow type combustor that merges into a single annulus, and a two-stage axial-flow turbine. The compressor-outlet mixer is used to obtain a velocity profile entering the combustor that provides a satisfactory radial temperature distribution at the turbine.

Afterburner

The afterburner configuration used in this investigation was similar to the most promising configuration developed in reference 1 and designated therein as the series C afterburner with the number 4 flame holder and corresponding optimized fuel pattern. The components of the afterburner consisted of a diffuser section, a combustion chamber with variable-area exhaust nozzle, a fuel distribution system, and a flame holder. Vortex generators were used on the inner cone at the diffuser inlet to minimize flow separation. The general arrangement and detailed dimensions of the afterburner shell and cooling shroud are shown in the sectional view of figure 2. Most of the afterburner combustion-chamber shell was provided with a uniform 1/2-inch annular passage for external air cooling while the exhaust nozzle and nozzle transition sections were water cooled. The required coolants were supplied from an outside source.

The fuel distribution system was installed in the diffuser section approximately 18 inches upstream of the flame holder. A total of 24 spray bars were equally spaced around the circumference of the afterburner, 12 long and 12 short tubes in alternate positions as sketched in figure 3. The spray bars were constructed of 1/4-inch Inconel tubing flattened to a thickness of about 1/8-inch. Holes of 0.020 inch diameter were drilled in the flattened sides of the spray bars, thus injecting fuel normal to the direction of gas flow. For a part of this investigation at high altitude only the 12 long spray bars were used. The 12 short spray bars were not removed but were separated from the fuel supply and blocked off.

The flame holder was of the three-ring V-gutter type with a blocked area of 35 percent. Details of the flame holder are shown in figure 4.

Ignition of the afterburner was accomplished by the hot-streak method wherein additional fuel was momentarily introduced at one location in the engine combustor to provide a flame through the turbine.

Installation

The engine and afterburner were installed in a 10-foot diameter altitude test chamber. A bulkhead in the test chamber, installed at a section corresponding to the engine inlet, was used to separate the inlet air flow from the exhaust gases and provide a means of maintaining a pressure differential across the engine. The exhaust gas from the jet nozzle was discharged into an exhaust diffuser. The pressure recovery in this diffuser was utilized to extend the maximum altitude limits of the facility. Combustion in the afterburner was observed through a periscope located in the exhaust duct behind the engine.

Instrumentation

Pressures and temperatures were measured at several stations throughout the engine and afterburner as indicated in figure 1. Air flow was determined from measurements of pressure and temperature at station 1. Afterburner-inlet conditions were determined from a comprehensive survey of pressure and temperature at the turbine outlet, station 5. The combustion temperature and thrust were determined from a survey of pressure at station 8 using a water-cooled rake located in a water-cooled section of constant diameter. For a part of the investigation the water-cooled rake was used to obtain samples of exhaust gas which were analyzed with an NACA mixture analyzer (ref. 2) to determine the fuel-air ratio distribution in the afterburner. Exhaust pressure was measured on the outside of the nozzle and in the plane of the exhaust-nozzle exit. Fuel flow was measured by means of a direct-reading calibrated rotameter.

Afterburner-shell temperatures were obtained with 6 thermocouples installed at each of two stations 6 inches apart located near the rear of the air-cooled portion of the afterburner shell. Cooling-air flow was measured using an orifice located in the supply line. Cooling-air temperatures were obtained from thermocouples located in plenum chambers at the inlet and outlet of the cooling passage.

PROCEDURE

Operational limits and performance at each flight condition were obtained by varying the afterburner fuel flow and jet-nozzle area while maintaining rated engine speed and the rated afterburner-inlet (turbine-outlet) temperature of 1625° R. Operational limits were obtained over a range of altitudes at a flight Mach number of 0.8. The lean fuel-air ratio limit was established by incipient blow-out observed through the periscope. The rich limit of operation was reached where the afterburner-inlet temperature was at the limiting or rated value with a wide open jet nozzle. Afterburner performance was obtained at altitudes from 10,000 to 55,000 feet and at flight Mach numbers of 0.6 to 1.0, thus covering a range of afterburner-inlet pressures of 510 to 3090 pounds per square foot. Inlet conditions to the engine at each flight condition corresponded to NACA standard atmosphere with 100 percent ram pressure recovery. Adequate cooling air and water were supplied to the afterburner shell from an external source to maintain the afterburner-shell temperature below 1550° F.

The symbols and method of calculating various parameters used in this report are shown in the appendix. The fuel used in the engine was clear unleaded gasoline (62 octane); that used in the afterburner was MIL-F-5624A grade JP-4.

RESULTS AND DISCUSSION

Operating Limits

2925 The operating range of the afterburner at a flight Mach number of 0.8 is shown in figure 5. The maximum altitude obtainable was limited by the capacity of the test facilities; however, operation at an altitude of 55,000 feet was possible at only one fuel-air ratio, indicating this to be the maximum altitude limit. The trend of a decreasing fuel-air ratio range with increasing altitude substantiates the conclusion that the maximum operating altitude is in this region. The trend of decreasing rich fuel-air ratio with altitude is typical of most engines and is due to the maximum afterburner gas temperature obtainable with a constant-area (wide-open) jet nozzle that arises from the Reynolds number effect on component efficiencies. Operation at stoichiometric afterburner fuel-air ratio was possible up to an altitude of 45,000 feet. It is expected that operation would have been possible at this fuel-air ratio at altitudes up to 55,000 feet or above had it been possible to further increase nozzle-exit area.

Performance Characteristics

The performance data for several flight conditions are presented in tabular form (table I) and are shown graphically in figures 6 through 9. The variations in combustion temperature and efficiency with afterburner fuel-air ratio are presented in figure 6. Performance data at an altitude of 45,000 feet and a flight Mach number of 0.8 were obtained at afterburner fuel-air ratios greater than the operational range (fig. 5). These data were obtained to more definitely establish the combustion temperature at stoichiometric fuel-air ratio by allowing the afterburner-inlet temperature to exceed 1625° R. Both the combustion temperature and efficiency were in good agreement with the data of reference 1, which are shown by the dashed line in figure 6.

A peak combustion temperature of 3900° R and a corresponding efficiency of 0.96 were obtained at flight conditions corresponding to afterburner-inlet pressures from 2540 to 2800 pounds per square foot. Peak temperatures occurred at about stoichiometric fuel-air ratio (0.0675) for all conditions except the highest pressure levels, where the peak temperature occurred at a richer mixture. Combustion efficiency (fig. 6(b)) reached a maximum value at a fuel-air ratio of about 0.055 and remained relatively constant with increasing fuel-air ratio. The efficiency decreased with increasing altitude (decreasing afterburner-inlet pressure) with a resultant reduction in combustion temperature. This typical trend of efficiency with pressure is shown in figure 7 for a fuel-air ratio of 0.052. As shown in this figure, a reduction in burner-inlet pressure from 3090 to 510 pounds per square foot lowered the efficiency from 0.95 to 0.61 with a resultant reduction in combustion temperature from 3560° to 2880° R.

This afterburner configuration produced smooth combustion under all flight conditions tested; however, the similar configuration of reference 1 was subject to a buzzing condition very near the lean blow-out fuel-air ratio at an afterburner-inlet pressure of about 2450 pounds per square foot. Lean blow-out was not obtained at this afterburner-inlet pressure with the configuration of this investigation, but operation at a low fuel-air ratio was obtained without encountering a buzzing condition. Combustion was also stable at a fuel-air ratio as low as 0.027 at an afterburner-inlet pressure of 3090 pounds per square foot.

The pressure losses in an afterburner must also be considered in a complete evaluation of afterburner performance. The variation of afterburner pressure loss ratio with afterburner fuel-air ratio is presented in figure 8. The friction total-pressure loss for the cold burner was 6 percent of the afterburner-inlet pressure. The pressure loss ratio increased with increasing fuel-air ratio because of the momentum pressure loss. The pressure loss with afterburning at the stoichiometric fuel-air ratio was about double the friction loss for the cold burner. There was no apparent trend of pressure loss ratio with flight-condition or afterburner-inlet pressure.

The effectiveness of the afterburner in terms of thrust is shown in figure 9(a) for the augmented jet thrust ratio and in figure 9(b) for the augmented net thrust ratio. The afterburner produced an augmented jet thrust ratio as high as 1.625 at an afterburner fuel-air ratio of 0.076 at the higher afterburner-inlet pressure levels which correspond to an augmented net thrust ratio of 2.03 at an altitude of 25,000 feet and a flight Mach number of 0.92. At lower pressure levels, the additional gain in augmented jet thrust obtained as the fuel-air ratio was increased above about 0.06 was small. The maximum augmented jet thrust ratio decreased with decreasing afterburner-inlet pressure as a result of the corresponding reductions in exhaust-gas temperature. Augmented jet thrust ratios greater than those measured may have been obtainable at altitudes of 50,000 and 55,000 feet by using a larger exhaust nozzle.

Effect of Fuel Distribution

At an altitude of 45,000 feet and a flight Mach number of 0.8, the fuel manifold pressure had decreased to approximately 25 pounds per square inch absolute at the stoichiometric fuel-air ratio. An attempt was made to improve the fuel penetration at this flight condition through increasing the fuel manifold pressure to 75 pounds per square inch absolute by using only the 12 long spray bars. A comparison of performance with the two fuel system configurations is presented in figure 10. Using only the 12 long spray bars resulted in a shift of the fuel-air ratio required for peak efficiency from 0.060 to about 0.100, with a resultant shift in fuel-air ratio for maximum combustion temperature from 0.068 to 0.078. The trends of increasing combustion efficiency of the 12 long spray bar configuration and the sustained efficiency of the 24 fuel spray bar configuration with increasing fuel-air ratio above

the stoichiometric mixture are unique with the method of calculating the efficiency. The efficiency, as defined in the appendix, is based on the ideal temperature rise which decreases above the stoichiometric mixture because of chemical energy remaining in the products of an ideal combustion. The most important effect of reducing the number of spray bars was the reduction in maximum temperature from 3420° to 3000° R. Penetration was insignificant in either case and the decrease in performance at a given fuel-air ratio was a result of circumferential and radial maldistribution. These results indicate the importance of providing a good fuel distribution in the afterburner and that such a distribution can be obtained only by using a large number of injection points rather than relying on penetration of the fuel jets into the air stream.

Fuel-Air Ratio Distribution

The fuel distribution was optimized in reference 1 by use of a temperature ladder comprising a 1/2-inch water-cooled Inconel tube spanning the diameter of the afterburner with pieces of 1/8-inch diameter welding rod of uniform length butt-welded to the tube. Local temperature profiles were observed by visual comparison of the color variations of the rods during afterburner operation. Since the criterion of a good fuel distribution system for the attainment of the maximum mean bulk gas temperature is a uniform fuel-air ratio distribution, in this investigation the fuel-air ratio distribution was checked during afterburner operation by direct measurement by use of a fuel-air ratio analyzer. Data from the fuel-air ratio analyzer using samples of the exhaust gas obtained from a survey at station 8, the exhaust-nozzle inlet, are presented in figure 11 for operation at an altitude of 35,000 feet and a flight Mach number of 1.0. The indicated fuel-air ratio distribution, which was fairly uniform, is an indication of the afterburner temperature profile that would be expected with this fuel system. Only a small additional increase in mean bulk temperature would be obtained near stoichiometric with a perfectly uniform fuel-air ratio profile (see fig. 6(a)).

Cooling-Air Requirements

In this investigation, the primary objective was to ascertain the performance over a wide range of flight conditions; the cooling air was therefore supplied from an outside source. The cooling-air flow supplied was adequate to permit operating with an allowable afterburner-shell temperature of 1550° F. During operation at an altitude of 35,000 feet and a flight Mach number of 1.0, the cooling-air requirements with parallel flow convective cooling were determined, and the data are presented in figure 12 as a function of combustion temperature for several average afterburner-shell temperatures. During this phase of the investigation the inlet cooling-air temperature was 83° F and the observed cooling-air temperature rise increased from 100° to 300° F as the combustion temperature was increased at a given average afterburner-shell temperature.

These data indicate that at the high combustion temperatures a large amount of cooling air was required for the convective system used herein. As much cooling air as 34 percent of the exhaust-gas flow was required to maintain an average afterburner-shell temperature of 1300°F at a combustion temperature of 3600°R . Minimizing the cooling-air flow requirements by increasing the average afterburner-shell temperature to the maximum safe operating temperature of the material is not representative of safe operation, since hot spots up to 250°F higher than the average were frequently encountered.

CONCLUDING REMARKS

An investigation was conducted to ascertain the operational limits of a high-temperature afterburner and to determine its performance over a wide range of flight conditions. Operational limits were obtained at a flight Mach number of 0.8 and performance data were obtained at altitudes from 10,000 to 55,000 feet and flight Mach numbers from 0.6 to 1.0.

The afterburner, designed to provide high combustion temperature, had a peak combustion temperature of 3900°R , representing a combustion efficiency of 0.96 and an augmented jet thrust ratio of 1.625 at an afterburner-inlet pressure of 2540 pounds per square foot. At these conditions, which compared with an altitude of 25,000 feet and a flight Mach number of 0.92, the augmented net thrust ratio was 2.03. A maximum operational altitude of 55,000 feet at a flight Mach number of 0.8 was obtained with an afterburner fuel-air ratio of 0.052. At this condition the combustion temperature was 2880°R , representing a combustion efficiency of 0.61. Maximum combustion efficiency was obtained at fuel-air ratios of about 0.055 and remained relatively constant with increasing fuel-air ratio. Peak combustion temperatures were obtained at the stoichiometric fuel-air ratio or at slightly richer mixtures.

The attainment of a high bulk gas temperature was dependent upon the attainment of a uniform fuel distribution. At an altitude of 45,000 feet and a flight Mach number of 0.8, the use of 24 instead of 12 spray bars resulted in an increase in temperature from 3000°R to 3420°R and a decrease in fuel-air ratio for maximum temperature from 0.078 to 0.068.

A severe cooling-air requirement was imposed on the convective shell cooling system used during this investigation. As much cooling air as 34 percent of the exhaust-gas flow was required to maintain an average afterburner-shell temperature of 1300°F at a combustion temperature of about 3600°R , which stresses the need for a more effective method of utilizing the cooling air.

Lewis Flight Propulsion Laboratory
National Advisory Committee for Aeronautics
Cleveland, Ohio

APPENDIX - CALCULATIONS

Symbols

The following symbols are used in this report:

A	cross-sectional area, sq ft
C_T	coefficient of thermal expansion
$C_{v,e}$	effective velocity coefficient
F_J	jet thrust, lb
F_N	net thrust, lb
f/a	fuel-air ratio
g	acceleration due to gravity, 32.17 ft/sec ²
H^O	sum of sensible enthalpy and chemical energy, Btu/lb
M	flight Mach number
m	mass flow, slugs/sec
P	total pressure, lb/sq ft
p	static pressure, lb/sq ft
R	gas constant, $\frac{1546 \text{ ft-lb}}{(\text{molecular weight}) (\text{lb}) (^{\circ}\text{R})}$
T	total temperature, $^{\circ}\text{R}$
V	velocity, ft/sec
W_a	air flow, lb/sec
W_F	fuel flow, lb/hr
W_g	gas flow, lb/sec
γ	ratio of specific heats
η	combustion efficiency

λ^0 a term accounting for difference between H^0 of carbon dioxide and that of water vapor in burned mixture and H^0 of oxygen removed from air by their formation

Subscripts:

a air
 b afterburner
 e engine
 ef effective
 g gas
 m fuel manifold conditions
 max maximum
 n exhaust-nozzle throat

Numbered subscripts as indicated on fig. 1

Methods of Calculation

Gas flow. - Engine-inlet air flow was calculated from measurements at station 1 using the following equation:

$$W_{a,1} = A_1 \sqrt{\frac{g}{R_{a,1}}} \frac{p_1}{\sqrt{T_1}} \left(\frac{p_A}{m \sqrt{gRT}} \right)_1^{-1} \quad (1)$$

Values of the static-pressure parameter $\frac{p_A}{m \sqrt{gRT}}$ were obtained from reference 3 assuming $\gamma_{a,1}$ to be 1.4. The gas flows at the entrance and exit of the afterburner were then determined by adding the appropriate fuel flow to the engine-inlet air flow.

Afterburner fuel-air ratio. - The afterburner fuel-air ratio is defined as the ratio of the afterburner fuel flow plus the unburned fuel from the engine combustor corrected for the difference in heating value of the two fuels to the unburned air entering the afterburner:

$$\left(\frac{f}{a} \right)_b = \frac{W_{f,b} + 1.013 (1 - \eta_e) W_{f,e}}{3600 W_{a,1} - \eta_e \frac{W_{f,e}}{0.0665}} \quad (2)$$

where 1.013 is the ratio of the lower heat of combustion of the engine fuel to that of the afterburner fuel and η_e is the ratio of the ideal to actual engine fuel flow required to heat the air flow from engine-inlet to afterburner-inlet temperature. The stoichiometric fuel-air ratio of the engine fuel is 0.0665.

Afterburner combustion temperature. - The combustion temperature was calculated from the gas flow and a pressure survey at station 8 using the continuity equation as follows:

$$T_8 = (A_8 C_T)^2 \frac{g}{R_{g,8}} \left(\frac{p_8}{w_{g,8}} \right)^2 \left(\frac{p_A}{m \sqrt{gRT}} \right)_8^{-2} \quad (3)$$

Values of the static-pressure parameter were obtained in the same manner as for the engine-inlet air flow using appropriate values for $\gamma_{g,8}$. The gas constant, $R_{g,8}$, and $\gamma_{g,8}$ were determined from the products of ideal combustion with no dissociation using the weighted averaging process and based on values obtained from reference 4. A water-gas reaction constant of 3.8 was assumed for mixtures greater than stoichiometric. The area A_8 was measured at room temperature and C_T was assumed to be unity, since the area at station 8 was water-cooled.

Afterburner combustion efficiency. - The combustion efficiency is defined as the ratio of the increase in energy of the exhaust gases in the afterburner to the ideal energy increase based on the afterburner fuel flow and the unburned engine fuel flow entering the afterburner:

$$\eta_b = \frac{w_{g,8} H^o_{g,8} - w_{g,5} H^o_{g,5} - \frac{w_{f,b}}{3600} \lambda^o_{b,m}}{w_{g,8} H^o_{g,T_{\max}} - w_{g,5} H^o_{g,5} - \frac{w_{f,b}}{3600} \lambda^o_{b,m}} \quad (4)$$

The term H^o was determined in the same manner as the gas constant in the calculation of combustion temperature. The value of $H^o_{g,T_{\max}}$

was determined from the ideal energy modified by an energy difference to account for the increase in chemical energy in the products of combustion due to the effect of dissociation. The value of this energy difference was based on data contained in reference 5.

Thrust. - The jet thrust was determined from the gas flow, the combustion temperature, and the ratio of exhaust-nozzle total pressure to altitude pressure P_8/p_0 by means of the following relations:

$$F_J = C_{v,e} \left[\frac{W_{g,8}}{g} V_n + A_n (p_n - p_0) \right] \quad (5)$$

$$F_J = C_{v,e} W_{g,8} \sqrt{\frac{R_{g,8} T_8}{g}} \left(\frac{V_{ef}}{\sqrt{gRT}} \right) \quad (6)$$

where

$$\frac{V_{ef}}{\sqrt{gRT}} = \frac{V_n}{\sqrt{gRT}} + \frac{p_n A_n}{m \sqrt{gRT}} - \frac{p_0 A_n}{m \sqrt{gRT}} \quad (7)$$

Values of the effective velocity parameter V_{ef}/\sqrt{gRT} were obtained from reference 3 and the ratio of exhaust-nozzle total pressure to altitude pressure P_8/p_0 using appropriate values of $\gamma_{g,8}$.

The normal jet thrust (no afterburning) was calculated in a similar manner using the conditions of the exhaust gases at the turbine outlet (station 5) and a total-pressure loss of 6 percent of P_5 for the nonoperative afterburner. The effective velocity coefficient $C_{v,e}$ was assumed to be unity in both cases. The augmented jet thrust ratio was then obtained by dividing the jet thrust by the normal jet thrust.

The net thrust was calculated from the jet thrust and inlet momentum:

$$F_N = F_J - mV_0 \quad (8)$$

where

$$mV_0 = p_1 A_1 \left(\frac{pA}{m \sqrt{gRT}} \right)_1^{-1} \left(\frac{V}{\sqrt{gRT}} \right)_0 \quad (9)$$

Values of $(V/\sqrt{gRT})_0$ were based on the desired ram ratio assuming γ to be 1.4. Values of the static-pressure parameter were the same as those used to determine the engine air flow. The augmented net thrust ratio was then obtained by dividing the net thrust by the normal net thrust.

REFERENCES

1. Conrad, E. William, and Campbell, Carl E.: Altitude Wind Tunnel Investigation of High-Temperature Afterburners. NACA RM E51L07, 1952.
2. Gerrish, Harold C., Meem, J. Lawrence, Jr., Scadron, Marvin D., and Colnar, Anthony: The NACA Mixture Analyzer and Its Application to Mixture Distribution Measurement in Flight. NACA TN 1238, 1947.
3. Turner, L. Richard, Addie, Albert N., and Zimmerman, Richard H.: Charts for the Analysis of One-Dimensional Steady Compressible Flow. NACA TN 1419, 1948.
4. Huff, Vearl N., Gordon, Sanford, and Morrell, Virginia E.: General Method and Thermodynamic Tables for Computation of Equilibrium Composition and Temperature of Chemical Reactions. NACA Rep. 1037, 1951. (Supersedes NACA TN's 2161 and 2113.)
5. Mulready, Richard C.: The Ideal Temperature Rise Due to the Constant Pressure Combustion of Hydrocarbon Fuels. M.I.T. Meteor Rep. UAC-9, Res. Dept., United Aircraft Corp., July 1947. (BuOrd Contract NOrd 9845.)

TABLE I. - HIGH-TEMPERATURE AFTERBURNER PERFORMANCE

Data run	Altitude, ft	Flight Mach number, M_0	Afterburner fuel-air ratio, $(f/a)_b$	Engine-inlet temperature, T_1 , OR	Engine-inlet pressure, P_1 , lb sq ft	Engine-inlet air flow, $W_{a,1}$, lb sec	Engine speed, rpm	Engine fuel-air ratio, $(f/a)_e$	Engine combustion efficiency, η_e	Afterburner-inlet temperature, T_6 , OR	Run
24 spray bar fuel											
70-27 28 29	10,000	0.6	0.0271 0.0404 0.0477	546 547 549	1856 1860 1855	48.81 48.79 48.42	12,505 12,502 12,509	0.0146 0.0148 0.0148	1.00 1.00 1.01	1620 1623 1632	1 2 3
91-9 8 7 6 5 4	15,000	0.6	0.0351 0.0422 0.0556 0.0609 0.0704 0.0787	503 503 502 501 501 500	1504 1507 1515 1506 1508 1510	42.73 42.99 43.00 42.95 43.01 43.18	12,498 12,486 12,502 12,494 12,511 12,509	0.0158 0.0157 0.0158 0.0157 0.0157 0.0159	0.99 .98 .98 .98 .98 .98	1641 1631 1632 1629 1633 1626	4 5 6 7 8 9
70-32 33 35 34 37 36	25,000	0.6	0.0481 0.0600 0.0669 0.0720 0.0876 0.0939	470 466 464 466 462 463	1000 1004 1003 1004 1000 1003	29.32 29.51 29.55 29.70 29.57 29.58	12,502 12,502 12,503 12,502 12,489 12,505	0.0163 0.0158 0.0162 0.0162 0.0164 0.0162	0.98 .98 .99 .98 .98 .99	1631 1596 1630 1632 1633 1626	10 11 12 13 14 15
83-1 2 3 4	25,000	0.92	0.0385 0.0499 0.0630 0.0750	506 504 505 504	1348 1355 1348 1349	37.69 37.97 37.69 37.69	12,497 12,506 12,502 12,499	0.0167 0.0166 0.0163 0.0155	0.99 .98 1.00 1.00	1632 1631 1622 1634	16 17 18 19
58-6 63-7 58-7 62-22 58-1 69-9 58-2 62-12 70-9 61-16 70-1 58-3 61-11 64-1 70-8 2 58-4 9 70-5 7 58-10 70-4 6 63-3 64-17 70-5	35,000	1.0	0.0384 0.0427 0.0429 0.0478 0.0501 0.0511 0.0551 0.0566 0.0595 0.0609 0.0609 0.0614 0.0621 0.0653 0.0660 0.0676 0.0687 0.0685 0.0687 0.0710 0.0738 0.0758 0.0768 0.0785 0.0813 0.0815 0.0850 0.0884 0.0888	472 476 472 475 473 472 474 472 475 474 473 475 477 475 473 476 473 480 473 477 476 477 478 473 475 475 478 476 475	947 937 949 942 939 954 946 951 943 958 942 939 948 948 958 935 935 936 945 942 935 944 939 935 940 938 935	28.18 27.27 28.00 28.10 27.61 28.30 27.47 28.04 27.76 27.57 27.21 27.56 27.85 27.49 28.11 27.46 27.38 28.15 27.54 27.23 28.10 27.28 27.27 27.83 27.42 27.46	12,502 12,505 12,502 12,503 12,511 12,477 12,515 12,511 12,497 12,506 12,484 12,502 12,511 12,490 12,509 12,508 12,505 12,505 12,503 12,503 12,503 12,503 12,509 12,506 12,507 12,506 12,506	0.0164 0.0166 0.0165 0.0168 0.0166 0.0168 0.0161 0.0165 0.0166 0.0162 0.0164 0.0162 0.0168 0.0166 0.0162 0.0167 0.0166 0.0166 0.0162 0.0162 0.0162 0.0162 0.0162 0.0167 0.0175 0.0162	0.85 .94 .94 .96 .96 .87 .98 .97 .96 .96 .94 .97 .95 .95 .94 .96 .96 .96 .96 .96 .96 .96 .96 .96 .96 .95 .93 .98	1608 1616 1606 1636 1626 1639 1622 1636 1629 1624 1626 1623 1634 1617 1649 1626 1636 1636 1624 1626 1636 1636 1626 1636 1636 1653 1628	20 21 22 23 24 25 26 27 28 29 30 31 32 33 34 35 36 37 38 39 40 41 42 43 44 45 46
62-33 58-16 17 18 19 20 21 84-4 21	40,000	0.8	0.0335 0.0392 0.0438 0.0505 0.0573 0.0634 0.0679 0.0710 0.0731	420 436 436 436 436 436 436 443 443	594 592 596 593 596 593 591 601 588	18.70 18.53 18.80 18.33 18.10 18.10 18.29 18.03 17.82	12,508 12,502 12,497 12,508 12,511 12,512 12,514 12,500 12,480	0.0180 0.0180 0.0176 0.0178 0.0178 0.0178 0.0180 0.0167 0.0172	0.92 .91 .92 .92 .91 .91 .92 .97 .96	1620 1628 1607 1621 1616 1616 1636 1624 1637	47 48 49 50 51 52 53 54 55
56-11 69-8 58-12 67-39 56-13 69-7 68-14 69-5 67-40 58-15 68-6 69-6 70-22 69-5 7 62-28 64-9 8 69-8	45,000	0.8	0.0394 0.0416 0.0444 0.0460 0.0504 0.0520 0.0556 0.0575 0.0579 0.0604 0.0606 0.0634 0.0668 0.0671 0.0690 0.0693 0.0726 0.0739 0.0767	439 445 439 447 445 448 448 444 460 439 441 434 434 438 440 440 460 443 440	472 468 463 462 465 467 467 463 467 465 467 466 468 467 475 465 459 464 467	14.49 14.15 14.56 14.14 14.35 14.11 14.35 14.18 13.94 14.59 14.22 14.16 14.24 14.21 14.30 13.98 13.69 13.94	12,499 12,492 12,514 12,503 12,500 12,497 12,505 12,531 12,494 12,512 12,508 12,514 12,494 12,494 12,443 12,500 12,500 12,467	0.0180 0.0192 0.0180 0.0185 0.0183 0.0188 0.0184 0.0188 0.0185 0.0191 0.0191 0.0190 0.0187 0.0186 0.0185 0.0185 0.0186 0.0189	0.89 .87 .91 .90 .89 .87 .88 .87 .89 .91 .88 .87 .89 .87 .87 .88 .88 .88 .85	1610 1649 1626 1657 1618 1637 1617 1627 1637 1634 1634 1637 1637 1631 1613 1624 1634 1644	56 57 58 59 60 61 62 63 64 65 66 67 68 69 70 71 72 73
62-31 30 84-6 62-29	50,000	0.8	0.0442 0.0521 0.0552 0.0582	429 433 450 437	367 363 450 370	11.32 10.21 10.93 11.27	12,500 12,500 12,497 12,508	0.0192 0.0197 0.0190 0.0193	0.84 .84 .86 .86	1606 1624 1634 1634	75 76 77 78
62-32	55,000	0.8	0.0522	465	288	8.52	12,518	0.0202	0.79	1622	79
12 spray bar fuel											
59-10 8 7 11 12 13 14 15	45,000	0.8	0.0573 0.0669 0.0758 0.0805 0.0813 0.0900 0.0905 0.0976	452 450 460 429 427 425 423 423	464 450 460 460 477 459 469 472	14.15 14.39 14.03 14.22 14.77 14.27 14.70 14.76	12,484 12,496 12,506 12,494 12,499 12,497 12,494 -----	0.0184 0.0180 0.0189 0.0189 0.0182 0.0188 0.0185 0.0184	0.87 .86 .86 .86 .90 .88 .88 .89	1612 1621 1619 1608 1614 1600 1610 1611	80 81 82 83 84 85 86 87

AT SEVERAL ALTITUDES AND FLIGHT MACH NUMBERS

Data run	Afterburner-inlet pressure, P_5 , lb sq ft	Afterburner combustion temperature, T_5 , °R	Afterburner combustion efficiency, η_b	Afterburner pressure loss ratio, $(P_5 - P_6)/P_5$	Jet thrust, F_j , lb	Augmented jet thrust ratio	Net thrust, F_N , lb	Augmented net thrust ratio	Run
injection system									
70-27	3074	2445	0.673	0.082	3578	1.241	2570	1.370	1
28	3109	3121	.861	.103	4048	1.334	3039	1.804	2
29	3077	3474	.931	.116	4196	1.460	3193	1.707	3
91-8	2788	2755	0.774	0.076	3610	1.325	2763	1.472	4
8	2793	3223	.896	.085	3936	1.440	3084	1.840	5
7	2806	3506	.886	.093	4130	1.512	3279	1.743	6
6	2790	3744	.936	.100	4255	1.561	3406	1.815	7
5	2773	3810	.926	.107	4312	1.583	3462	1.847	8
4	2824	3885	.980	.119	4444	1.615	3591	1.891	9
70-32	-----	3288	0.851	-----	2706	-----	-----	-----	10
33	-----	3533	.867	-----	2799	-----	-----	-----	11
35	-----	3678	.882	-----	2902	-----	-----	-----	12
34	-----	3623	.859	-----	2910	-----	-----	-----	13
37	-----	3500	.883	-----	2923	-----	-----	-----	14
36	-----	3403	.890	-----	2911	-----	-----	-----	15
83-1	2532	2937	0.792	0.104	3785	1.366	2657	1.603	16
2	2538	3485	.917	.116	4150	1.496	3045	1.824	17
3	2531	3829	.960	.122	4357	1.586	3259	1.976	18
4	2577	3940	.972	.122	4534	1.626	3431	2.036	19
58-6	1807	2959	0.819	0.090	2957	1.390	2105	1.651	20
53-7	1768	3061	.805	.100	2899	1.411	2071	1.686	21
58-7	1806	3143	.851	.095	3029	1.437	2182	1.729	22
18	1829	3255	.855	.094	3132	1.456	2282	1.754	23
62-22	1780	3232	.796	.107	3031	1.450	2196	1.750	24
58-1	1836	3434	.885	.101	3230	1.494	2374	1.818	25
69-9	1735	3461	.858	.112	3093	1.505	2261	1.850	26
58-2	1827	3584	.900	.105	3278	1.532	2430	1.882	27
62-12	1783	3481	.836	.112	3185	1.515	2341	1.861	28
70-9	1745	3593	.876	.120	3182	1.535	2347	1.894	29
61-18	1775	3642	.898	.116	3181	1.548	2357	1.910	30
70-1	1754	3564	.862	.120	3174	1.529	2339	1.895	31
58-5	1820	3638	.889	.108	3288	1.549	2442	1.914	32
61-11	1777	3637	.872	.118	3216	1.554	2383	1.926	33
64-1	1804	3678	.888	.115	3320	1.566	2470	1.943	34
70-8	1748	3619	.852	.125	3200	1.548	2366	1.916	35
2	1744	3649	.881	.120	3210	1.566	2383	1.948	36
58-4	1785	3638	.861	.114	3238	1.568	2404	1.931	37
70-3	1817	3548	.890	.116	3307	1.545	2455	1.905	38
7	1746	3681	.845	.132	3168	1.553	2357	1.929	39
58-10	1747	3631	.863	.128	3219	1.569	2392	1.953	40
70-4	1828	3516	.826	.117	3326	1.547	2475	1.904	41
6	1749	3530	.858	.136	3197	1.568	2366	1.935	42
63-3	1749	3536	.862	.132	3210	1.562	2383	1.939	43
64-17	1792	3580	.830	.133	3240	1.530	2398	1.881	44
70-5	1779	3548	.861	.126	3264	1.557	2429	1.925	45
11	1751	3363	.850	.134	3187	1.536	2353	1.901	46
82-33	1189	2703	0.758	0.096	1750	1.311	1310	1.464	47
58-16	1178	2890	.748	.087	1788	1.352	1344	1.531	48
17	1166	3068	.802	.107	1866	1.408	1400	1.618	49
18	1170	3361	.815	.109	1891	1.454	1452	1.684	50
19	1163	3444	.839	.115	1918	1.498	1484	1.754	51
20	1160	3535	.847	.118	1946	1.523	1512	1.791	52
21	1175	3608	.815	.121	1980	1.513	1542	1.770	53
84-4	1125	3352	.760	.142	1844	1.472	1408	1.723	54
11	1141	3547	.836	.138	1917	1.519	1486	1.788	55
58-11	898	2755	0.686	0.107	1339	1.330	991	1.505	56
89-8	891	3028	.802	.112	1372	1.376	985	1.615	57
58-12	890	2869	.681	.105	1387	1.407	1037	1.545	58
87-39	947	3043	.748	.113	1424	1.381	1081	1.571	59
58-13	898	3149	.761	.119	1438	1.425	1093	1.646	60
89-7	878	3333	.828	.124	1432	1.454	1045	1.747	61
58-14	895	3262	.756	.125	1459	1.450	1114	1.695	62
89-5	874	3447	.835	.132	1460	1.480	1073	1.791	63
87-40	864	3320	.772	.134	1406	1.444	1067	1.682	64
58-15	903	3213	.717	.122	1466	1.442	1135	1.689	65
89-6	886	3391	.796	.128	1446	1.478	1103	1.738	66
89-8	874	3409	.788	.133	1458	1.474	1071	1.779	67
70-22	871	3402	.741	.138	1443	1.454	1102	1.691	68
89-5	870	3401	.767	.142	1458	1.475	1117	1.726	69
89-7	881	3391	.770	.139	1484	1.487	1120	1.748	70
62-28	877	3441	.788	.140	1453	1.493	1113	1.758	71
84-9	871	3368	.768	.141	1437	1.473	1101	1.720	72
8	876	3347	.765	.142	1445	1.469	1108	1.714	73
89-8	854	3365	.792	.122	1411	1.488	1081	1.747	74
62-31	691	2845	0.676	0.119	1057	1.344	786	1.524	75
30	683	3049	.695	.129	1085	1.386	817	1.585	76
84-8	688	3072	.677	.153	1033	1.369	767	1.570	77
62-29	684	3146	.695	.145	1094	1.396	824	1.605	78
62-32	510	2886	0.611	0.141	773	1.334	562	1.525	79
injection system									
59-10	883	2898	0.497	0.110	1311	1.330	966	1.509	80
8	905	2967	.581	.115	1405	1.401	1055	1.642	81
7	887	2995	.649	.115	1407	1.426	1069	1.652	82
11	888	2933	.688	.117	1421	1.428	1083	1.647	83
12	915	2912	.664	.106	1477	1.431	1127	1.653	84
13	902	2956	.744	.123	1462	1.458	1124	1.680	85
14	914	2930	.741	.121	1497	1.449	1150	1.677	86
15	920	2859	.767	.119	1505	1.449	1157	1.678	87

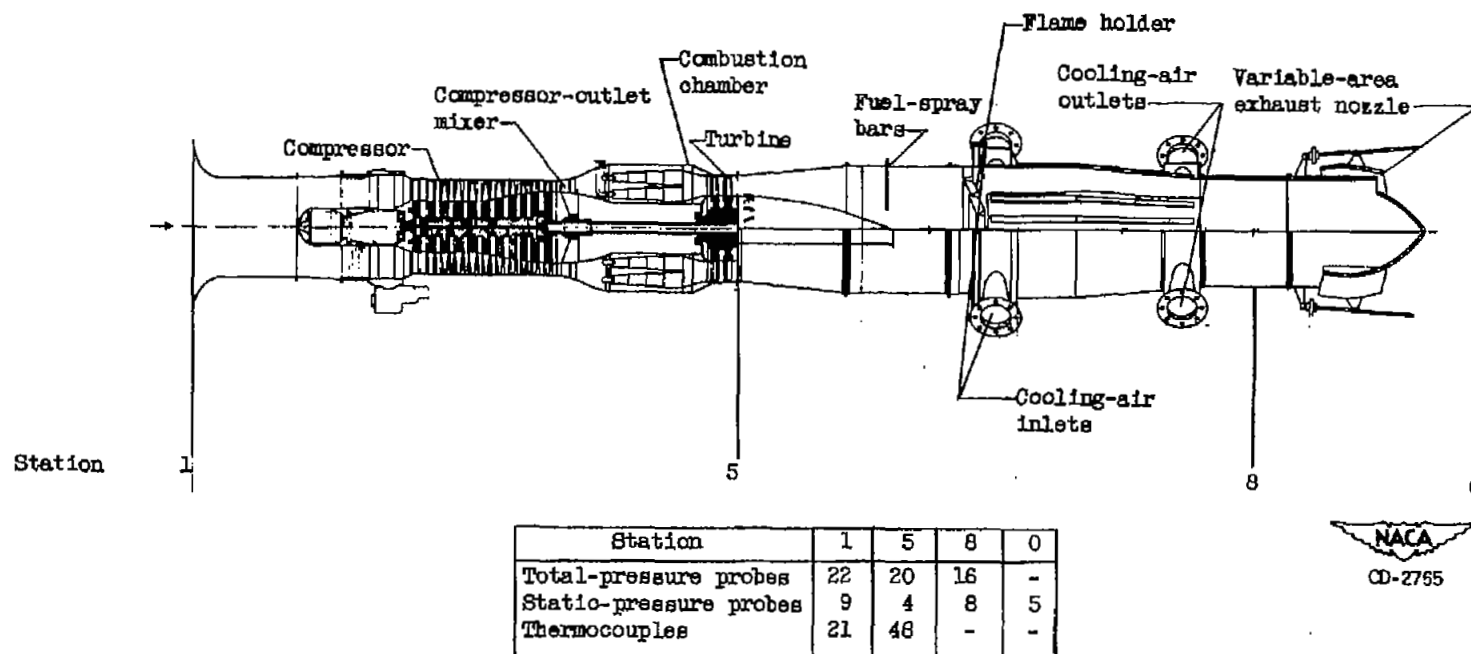


Figure 1. - Sectional view of engine showing instrumentation stations.

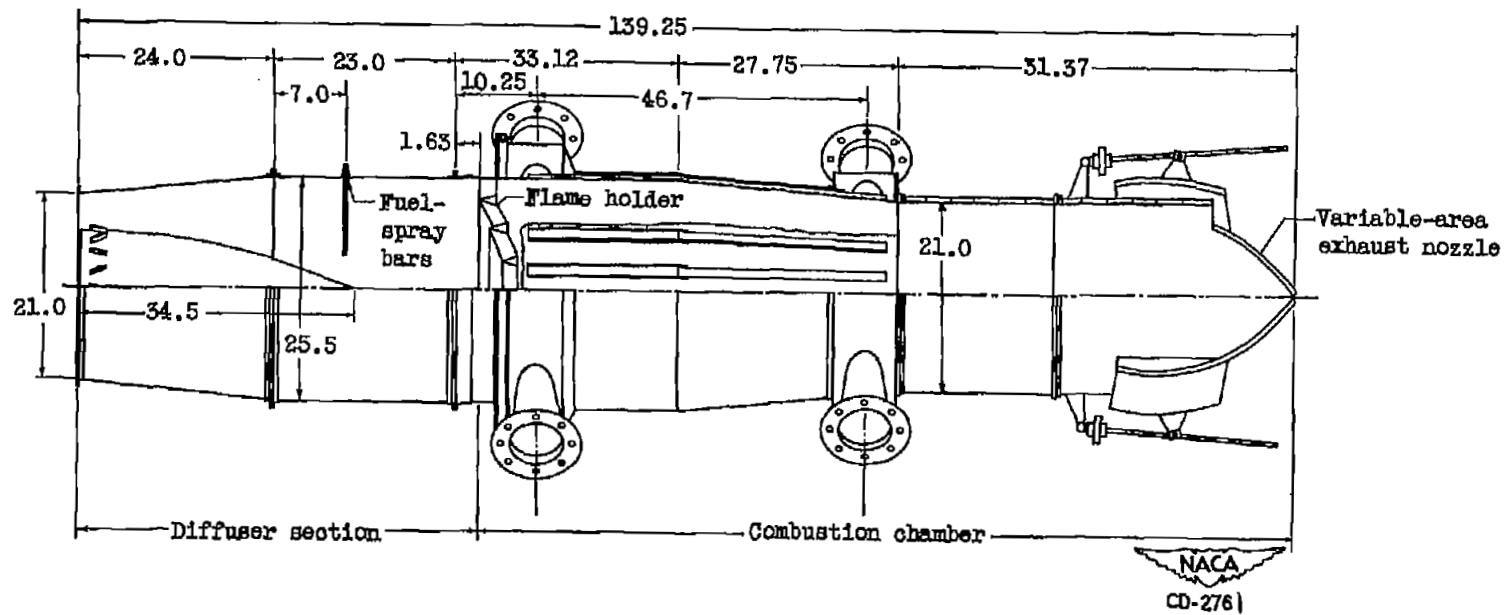


Figure 2. - Sectional view of afterburner. (All dimensions are in inches.)

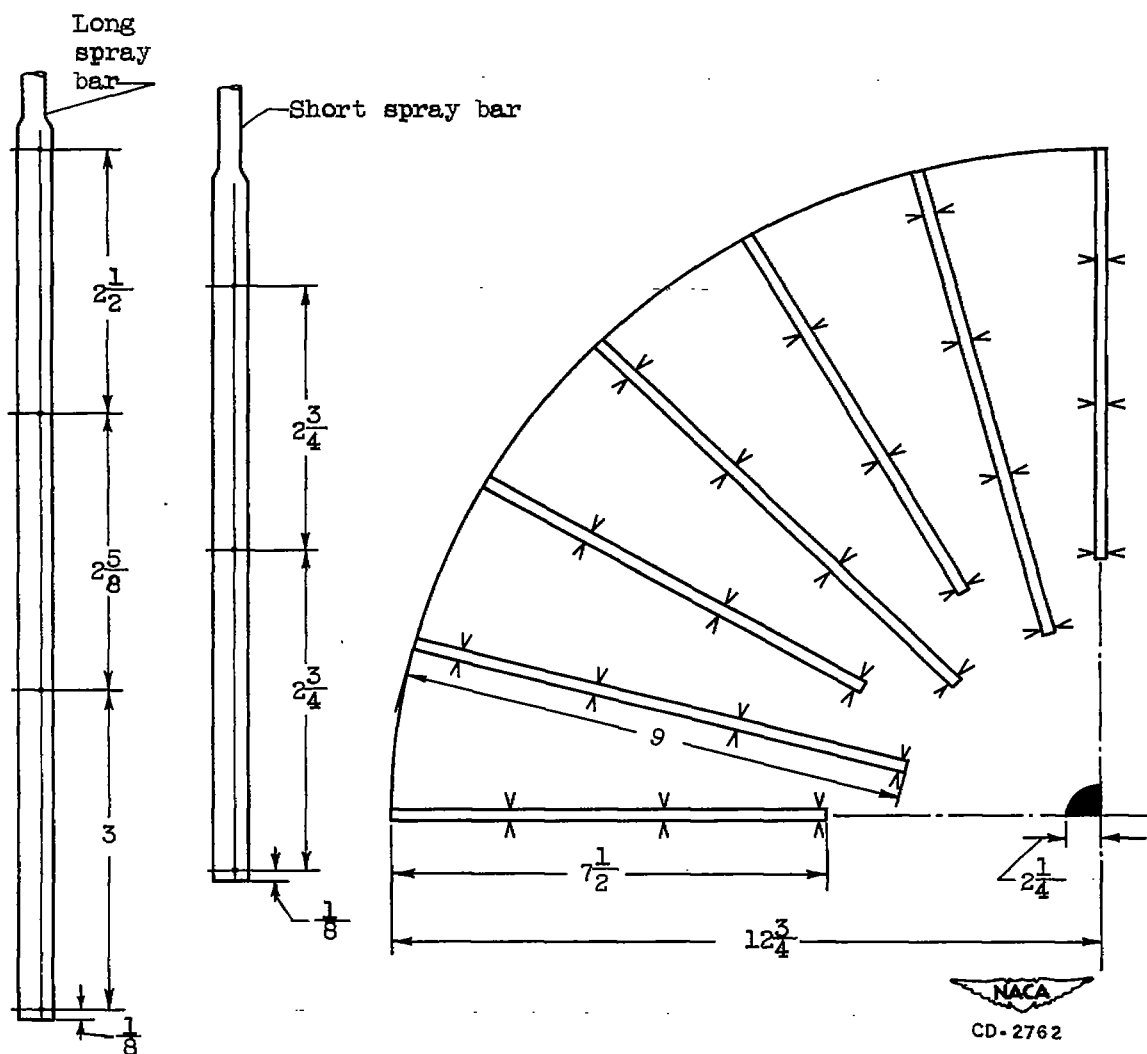
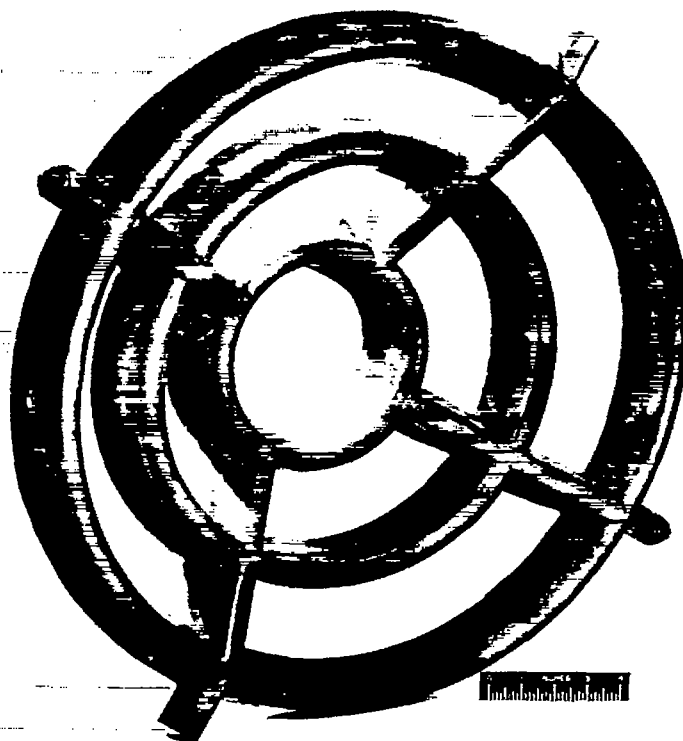
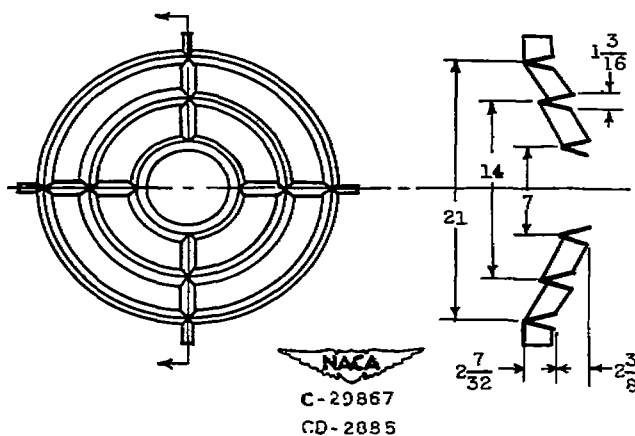


Figure 3. - Details of afterburner fuel-distribution system.
Diameter of all holes, 0.020 inch. (All dimensions are in inches.)



(a) View of flame holder.



(b) Flame-holder dimensions. (All dimensions are in inches.)

Figure 4. - Details of afterburner flame holder. Area blockage, 35 percent.

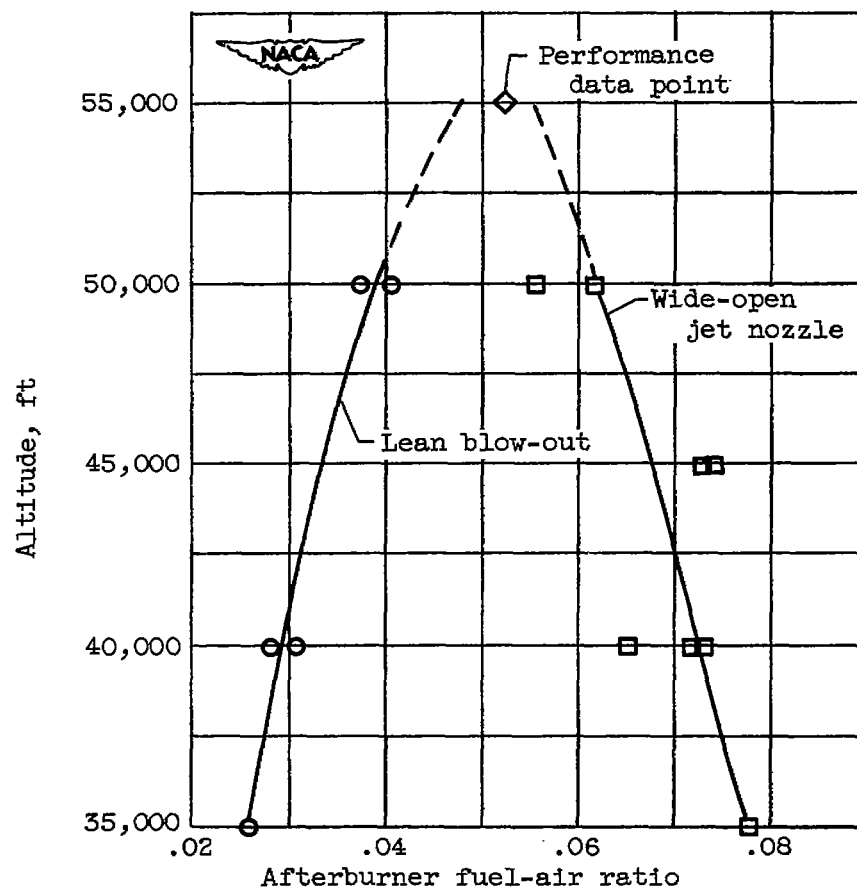
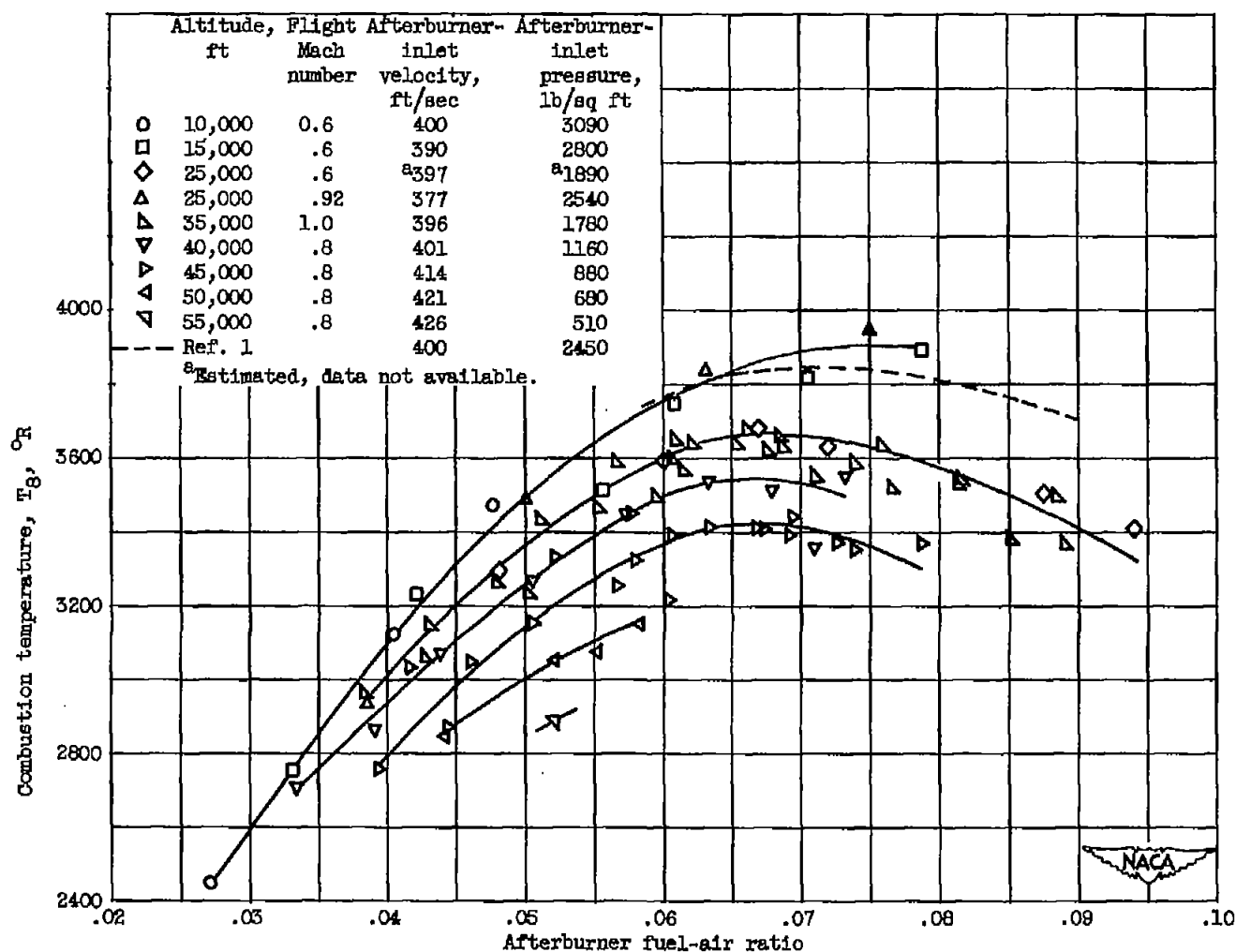
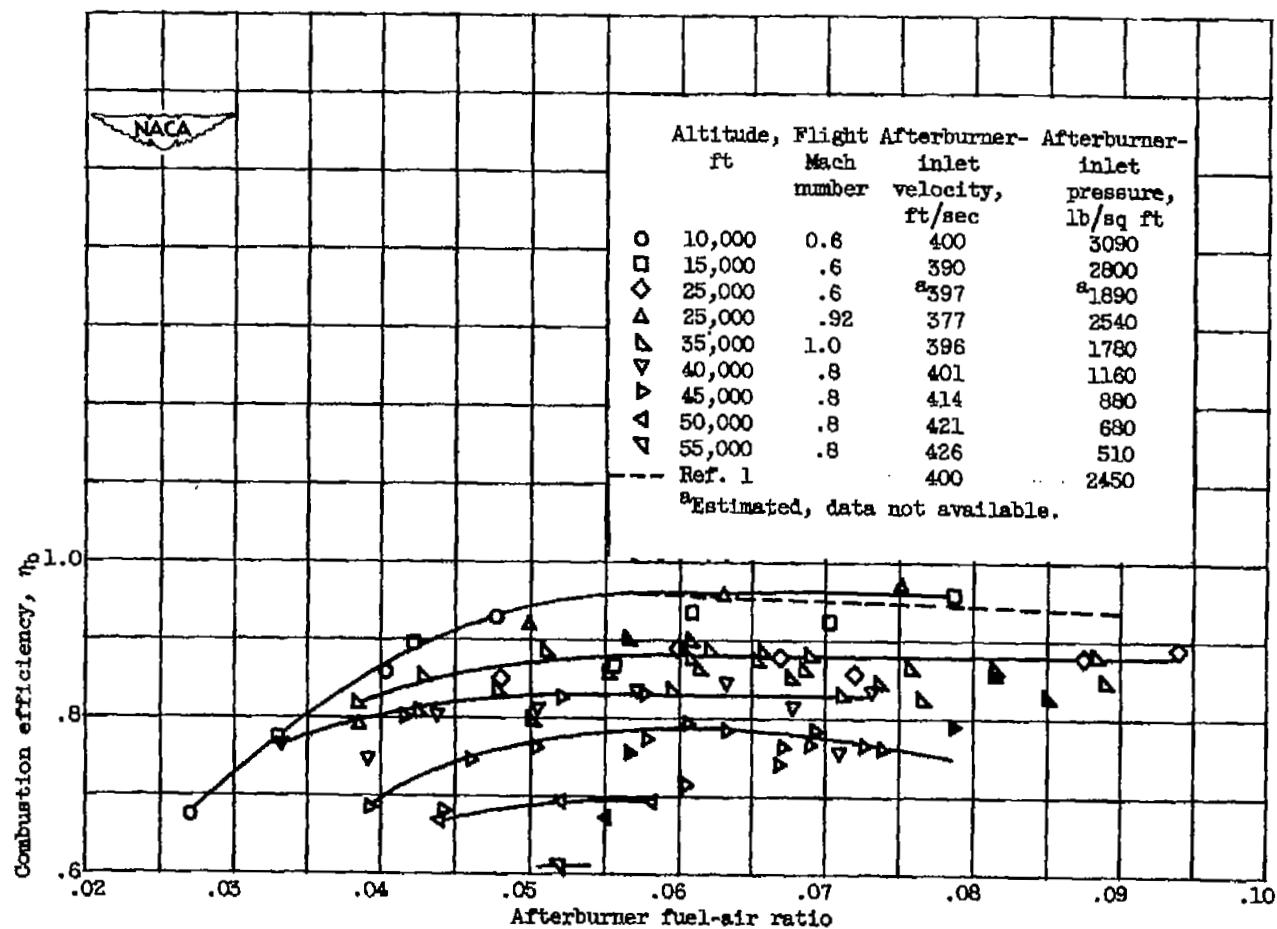


Figure 5. - Operating range of afterburner at flight Mach number of 0.8. Afterburner inlet temperature, 1625° R.



(a) Combustion temperature.

Figure 6. - Variation of combustion temperature and efficiency with afterburner fuel-air ratio at several flight conditions. Afterburner-inlet temperature, 1825° R.



(b) Combustion efficiency.

Figure 6. - Concluded. Variation of combustion temperature and efficiency with afterburner fuel-air ratio at several flight conditions. Afterburner-inlet temperature, 1625° R.

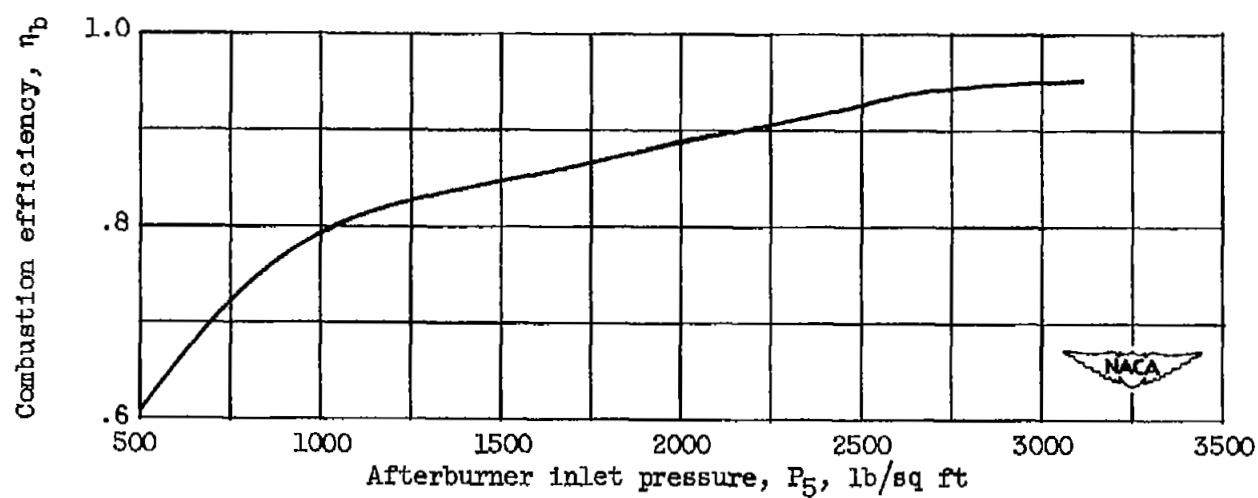


Figure 7. - Variation of combustion efficiency with afterburner-inlet pressure.
Afterburner fuel-air ratio, 0.052; afterburner-inlet temperature, 1625° R.

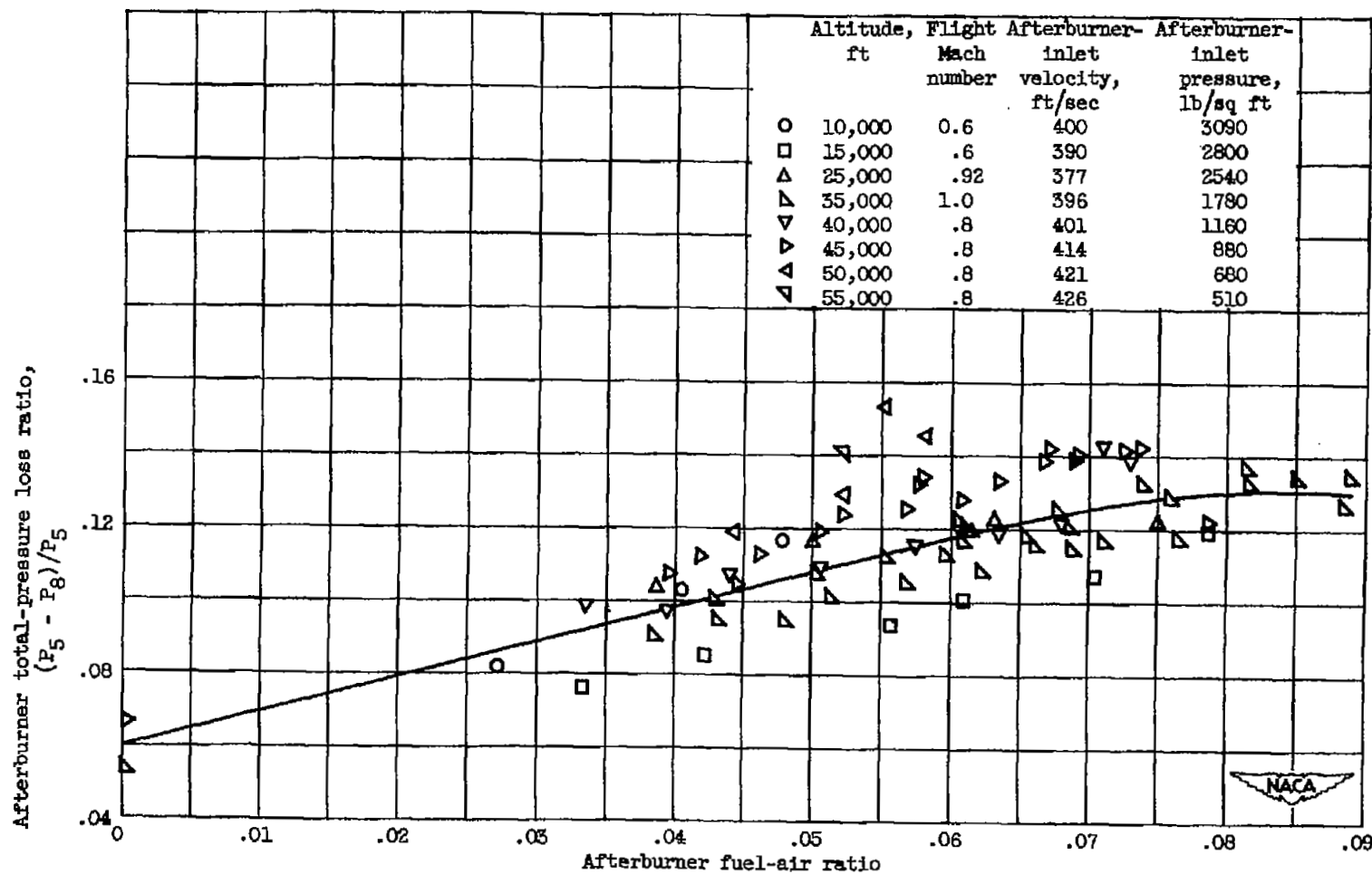
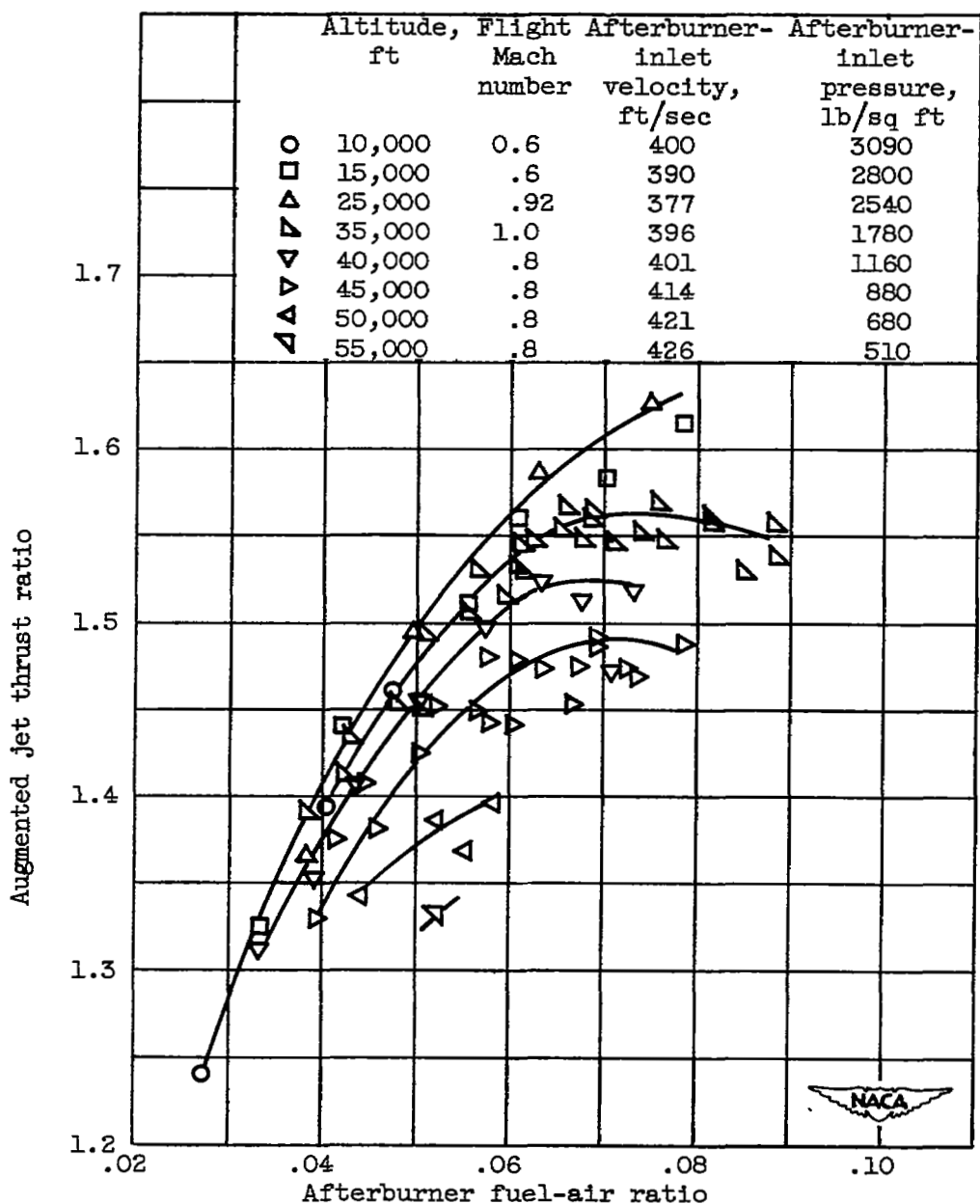
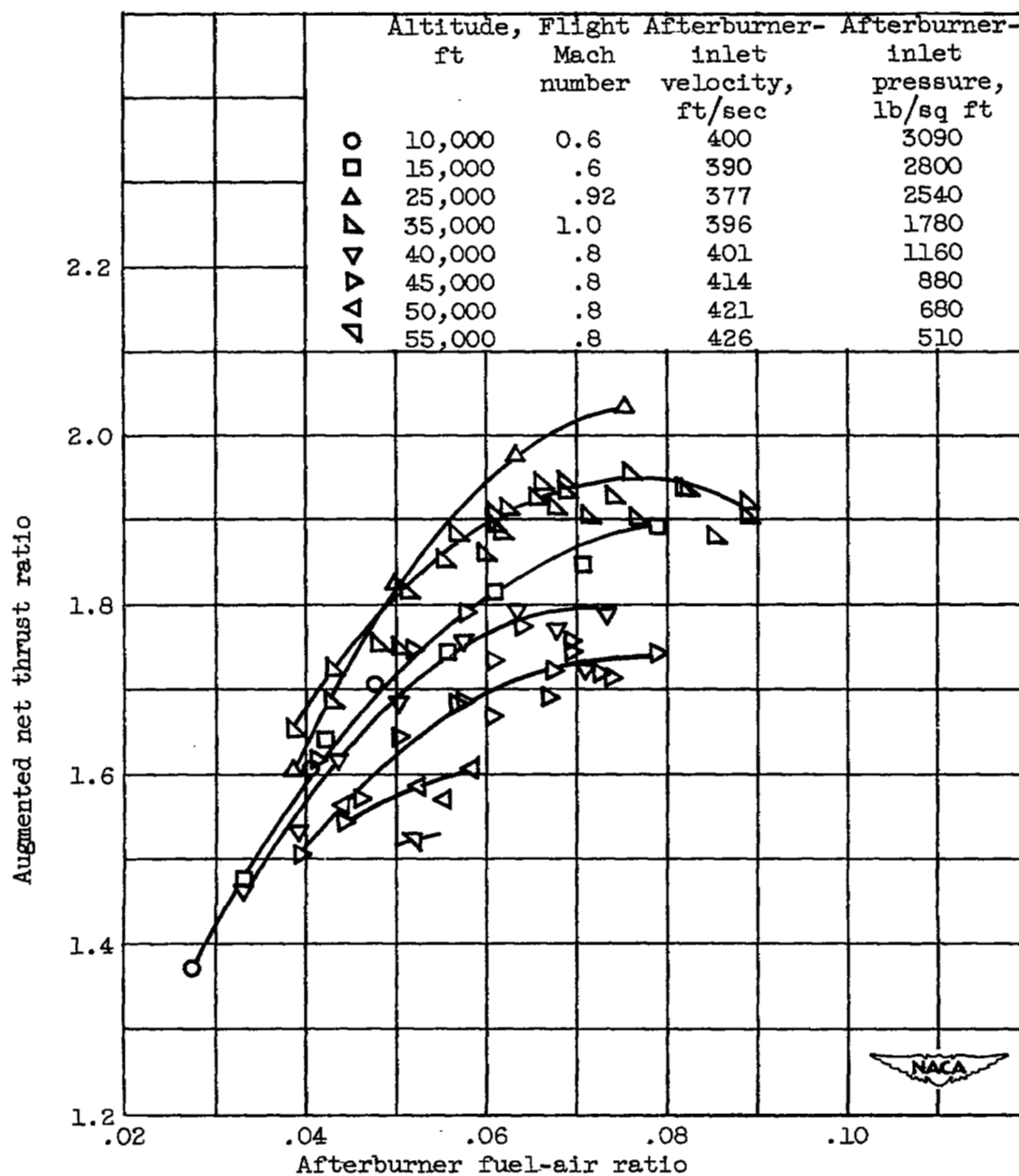


Figure 8. - Variation of afterburner total-pressure loss ratio with afterburner fuel-air ratio at several flight conditions.



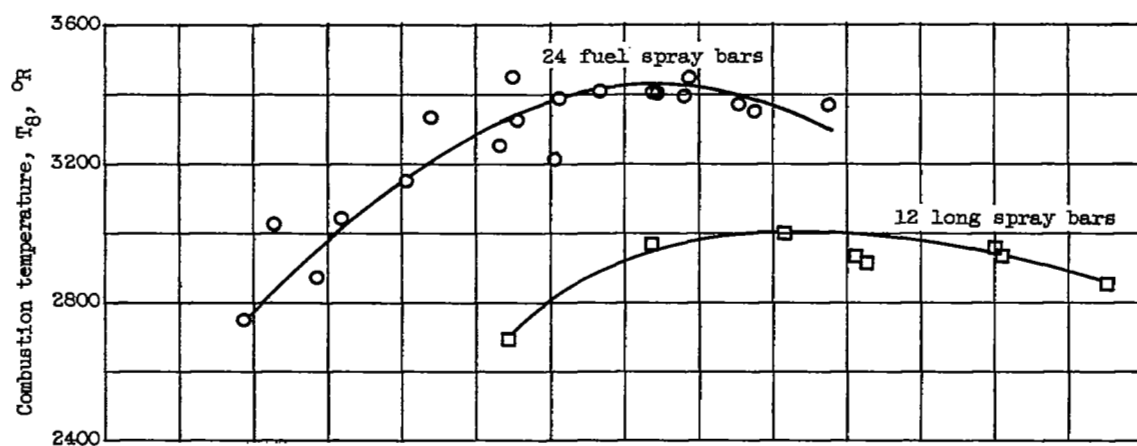
(a) Jet thrust.

Figure 9. - Variation of augmented thrust ratio with afterburner fuel-air ratio at several flight conditions.

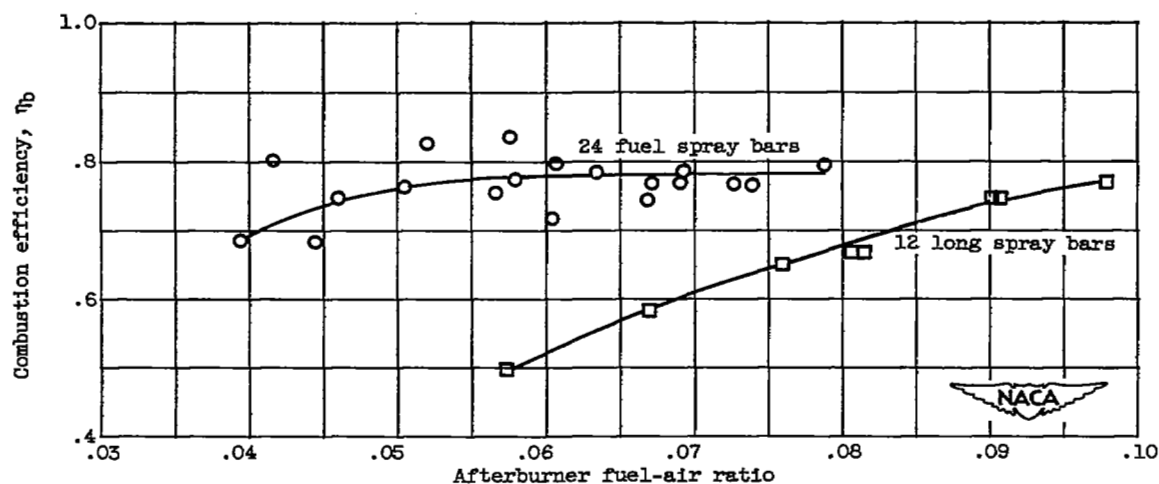


(b) Net-thrust.

Figure 9. - Concluded. Variation of augmented thrust ratio with afterburner fuel-air ratio at several flight conditions.



(a) Combustion temperature.



(b) Combustion efficiency.

Figure 10. - Variation of combustion temperature and efficiency with afterburner fuel-air ratio for two fuel system configurations. Altitude, 45,000 feet; flight Mach number, 0.8.

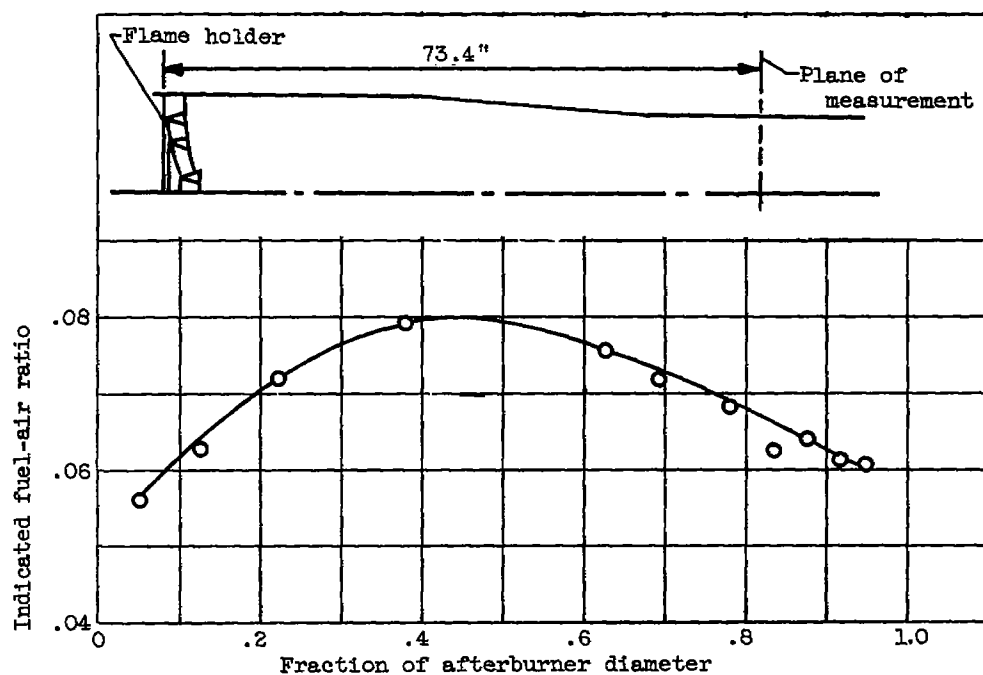


Figure 11. - Indicated fuel-air ratio distribution across afterburner. Altitude, 35,000 feet; flight Mach number, 1.0; measured fuel-air ratio, 0.069.

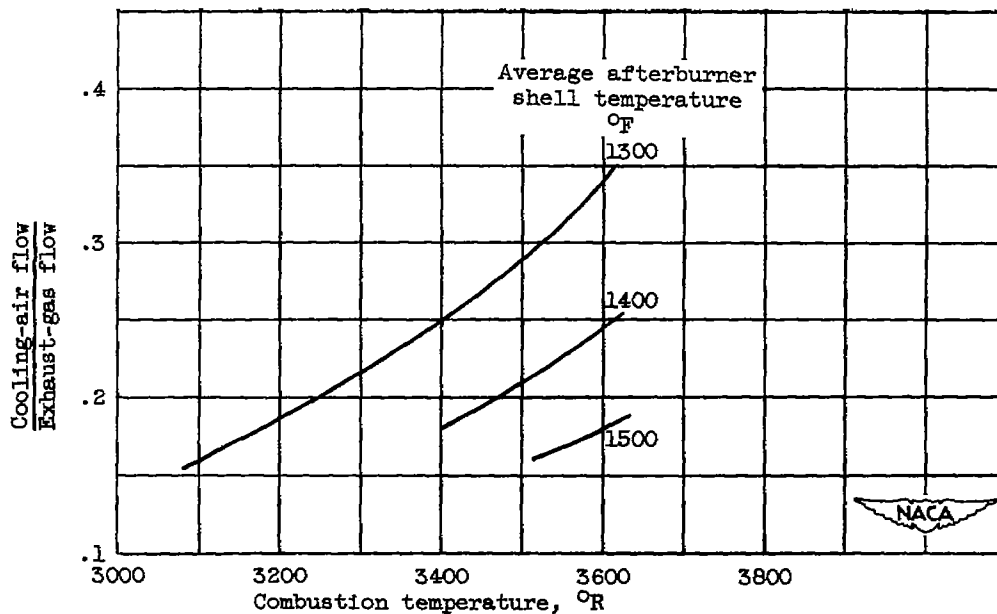


Figure 12. - Parallel flow cooling-air requirements of high-temperature afterburner. Altitude, 35,000 feet; flight Mach number, 1.0; inlet-cooling-air temperature, 83° F; cooling-air temperature rise, 100-300° F.

SECURITY INFORMATION

[REDACTED]



[REDACTED]